Chapter 8

Geophysical Monitoring of CO_2 Injection at Citronelle Field, Alabama

Shen-En Chen and Yangguang Liu

Additional information is available at the end of the chapter

http://dx.doi.org/10.5772/intechopen.78386

Abstract

Carbon dioxide (CO_2) injection at the Citronelle oil field in Alabama has been deployed to determine the feasibility of carbon storage and enhanced oil recovery (EOR) in the depleted oil field. Citronelle is a small size city right above the oil field, hence, to detect geohazard risks, geophysical testing method using wireless sensor, and passive seismic technique is used: the non-intrusive measurements were made at well sites along two linear arrays. The outcomes of the geophysical monitoring at the Citronelle oil field are shear-wave velocity profiles that are correlated to the static stress distribution at different injection stages. Injection history interpretation using the stress wave monitoring indicates that CO_2 injection resulted in the stressing of the strata.

Keywords: geophysical testing, Citronelle oil field, CO_2-EOR, carbon sequestration, strata stressing

1. Introduction

Carbon dioxide (CO_2) is a greenhouse gas, and the relationship between global warming and greenhouse gases has become more and more of a concern to the scientific community [1–3]. Because there is continual rise in what is already a high concentration of CO_2 in the atmosphere, it is imperative that a viable solution be implemented. Carbon capture and geologic storage is a promising method for reducing the concentration of CO_2 in the Earth's atmosphere [4–7]. The technology involves collecting CO_2 from an emission heavy source, compressing and transporting the CO_2 to a qualified site and injecting the now supercritical CO_2 at high-pressure into the reservoir. The qualified storage reservoir must satisfy stringent geological storage criteria, which may include anticline, porosity, permeability, void volume, pressure

limits, seepage characteristics, and cap rock characteristics. The reservoir should be sufficiently distanced from any potable groundwater acquifers to avoid contamination issues. Using underground depleted oil and gas reservoirs as CO_2 storage sites may have secondary advantages of enhanced oil recovery (EOR) or enhanced gas recovery (EGR) [8–10]. The additional fossil resources recovery can provide the economic incentives for CO_2 storage. Currently, there are several hundreds of oil field injection sites worldwide and in the US [11, 12].

While no CO_2 leakage has been reported at any injection sites, it is important to instate careful monitoring programs for such practices to avoid potential geohazards. Recent studies of remote sensing data indicate that some of the injection sites may have experienced surface deformation [13–15]. Effective monitoring programs should be adopted at the injection sites in order to detect changes in geological formation (geomorphology) and the presence and migration of CO_2 within the storage reservoir [16–19].

Since 2010, CO_2 has been injected for possible CO_2-EOR at a highly heterogeneous and discontinuous sandstone reservoir of the Citronelle oil field, Alabama. Citronelle oil field is a matured oil reservoir and an ideal site for CO_2-EOR and sequestration, from both reservoir engineering and geological perspectives [20, 21]. The Citronelle oil field is located about 50 km north of Mobile on the crest of the Citronelle Dome, which is a giant salt-cored anticline in the eastern

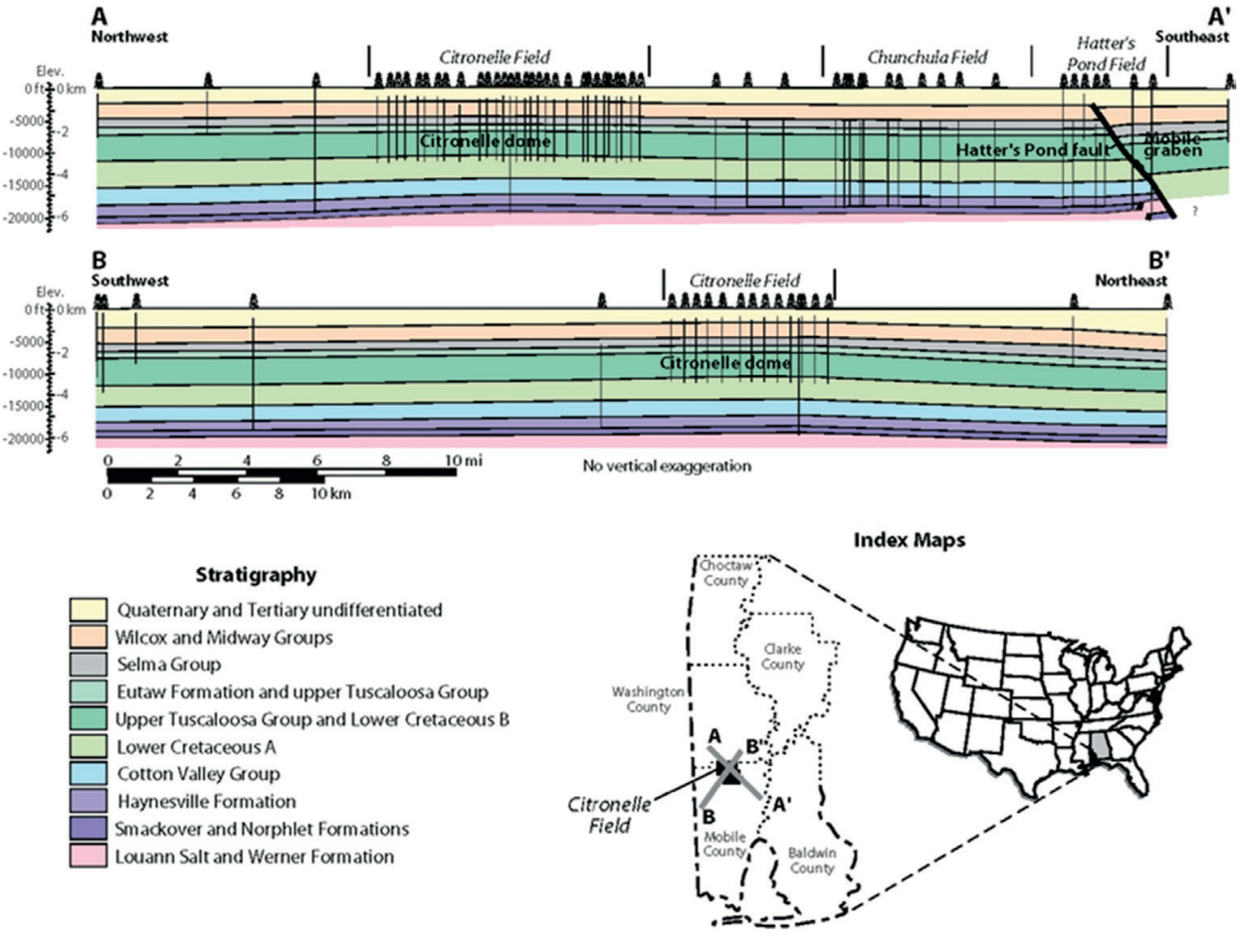

Figure 1. Structural cross sections showing Citronelle dome and location of Citronelle field.

http://dx.doi.org/10.5772/intechopen.78386

Figure 2. Typical locations of the oil wells at Citronelle, Alabama.

Mississippi Interior Salt Basin (**Figure 1**). The field covers an area of 16,400 acres directly below the city of Citronelle. In 1955, oil was first discovered by the Gulf Oil Company in the Zack Brooks Drilling Company No. 1 Donovan well. Since then, over 500 wells have been drilled and cumulative oil production has exceeded 169 million barrels at Citronelle Field.

Citronelle is a small city with a population of 3900 (2010 consensus). With most of the oil wells integrated into the cityscape, possible geohazards such as CO_2 leaks can be detrimental to the local citizens, live stocks, and the environment. Some of the wells exist within residents' backyards and farmlands (**Figure 2**). To detect risks of geohazards and monitor the injection process, geophysical testing has been performed at the site. This paper reports the outcomes of the field tests due to CO_2 injection into the Unit B-19-10 #2 well (Permit No. 3232). The goal of the geophysical testing is to establish possible relationships between shear-wave velocity profiles and the static stress distribution before, during and after the injection. Such relationships are helpful in understanding the site condition changes due to the injection activity.

2. Geophysical monitoring strategies

The intent of the carbon injection is to explore the feasibility of EOR in the tertiary production of an existing oil reservoir, as well as the potential of subsequent CO_2 sequestration. The geophysical monitoring strategy is used to assess the site geostability and potential geohazards. Site geostability for mineral extractions can be associated either with the site geological conditions pertaining to sustained production or with the large geological deformations such

as land subsidence or landslides. In the context of the current study, the association is with the latter definition. The key purpose of a geostability analysis is to determine the possibilities of significant geohazards due to formation instabilities, which may result from the CO_2-oil replacement in the Rodessa formation.

Geo-instability of an oil-producing stratum can result from the collapse of voids during the oil extraction process. The repercussions may include global subsidence, localized straining and possible microtremors to earthquakes. **Figure 3** shows a schematic of the geomaterial straining at an oil extraction well. The hypothesis is that as oil is being depleted, the surrounding geomedium may experience straining due to interfacial shear stresses resulting from the settlement and collapse of the strata. Geostability in a narrow oil field within a deep stratum, such as the Citronelle oil field, is typically not a major concern since relatively small settlement is anticipated. The geo-instability concerns in such cases can be generalized as compressibility potential assessment as well as localized stability projection.

The compression or settlement issue may involve both local elastic settlement (non-permanent deformation) and long-term creep (long-term deformation due to sustained loading). Elastic settlement is instantaneous and is a function of the weight of overburden above the layer of interest. For an oil-producing layer, elastic settlement is also a function of the system pressurization, where pressure is kept to ensure the injection fluids remain in the oil layer. Creep is difficult to assess since it is a function of time. Current geostability analysis does not include considerations of thermoelastic effects or micro-poroelastic effects for the pressurized system, for example, the Biot's equations. The rationale is that the difficulties in establishing geomaterial properties based on current geophysical measurements and assumed values only allow a grossly simplified bulk material analysis. As a result, the extensive works by Biot on poroelasticity has been greatly simplified.

Stresses in geomaterials are derived essentially from the self-weight of the overburden materials (predominantly the geo-matrix), the liquid within the voids (pore water pressure), and

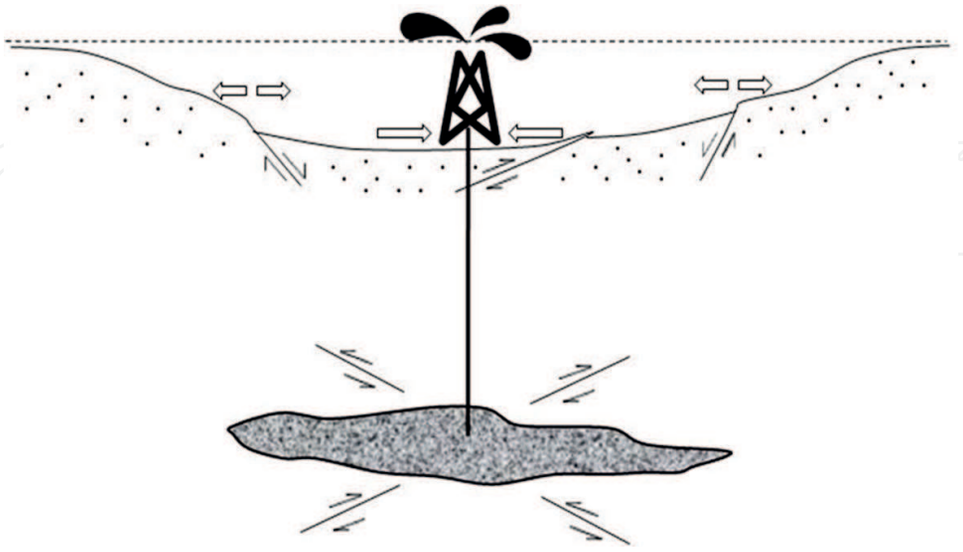

Figure 3. Poroelastic stresses due to extensive oil extraction (hollow arrows indicate surface strains and line arrows indicate interplanar shear stresses).

http://dx.doi.org/10.5772/intechopen.78386

the externally induced pressures. Hence, the total stress within the geomaterial system is equal to the summation of stress within geo-matrix and pore water pressure. The geostability study considers the effective stress, σ′, which is defined as the stress carried by geomaterial skeletons and not pore water that causes elastic deformation of the oil-producing layer:

$$\sigma' = \sigma - \mu \tag{1}$$

where σ is the vertical total stress derived from unit weight of material and μ is the pore pressure. Neglecting thermal effects, the effective stress equation is further modified to include injection pressure $\sigma_{injection}$:

$$\sigma'' = \sigma' - (\sigma_{injection} - \mu) \tag{2}$$

The effective stress pressure is then used to compute the producing layer elastic deformation (non-permanent settlement) using simplified computation of rock bulk modulus (P-wave modulus), M [22]:

$$M = \rho V_p^2 \tag{3}$$

where ρ is the rock density, V_p is the P-wave velocity derived from geophysical testing conducted at Citronelle.

2.1. Geophysical testing at Citronelle field

Micro-seismicity tests have been successfully applied to address specific issues in the oil and gas industry [23, 24]. The basic principle of passive seismic monitoring is to detect small movements (regarded as microseismic events) from unknown seismic sources that can be recorded on geophones placed on site. Contrast to active geophysical testing, the passive seismic monitoring is a testing method that does not rely on a source of ground excitation. The main advantage of the passive monitoring is that it can be carried out at any time and does not require regulated field access. The disadvantage of passive sensing is the uncertainty introduced due to the lack of controlled input energy, which can result in both poor data sensitivity and poor detection accuracy.

A modified passive sensing Refractive Microtremor (ReMi) technique, Derivative of ReMi (DoReMi), as discussed below, is used at the Citronelle oil field, Alabama [25]. To improve mobility and avoid the cumbersome wiring, wireless triaxial micro-electro-mechanical system (MEMS) accelerometers have been used for the field testing. The MEMS sensors are encased in hard metal boxes and buried into the ground at sufficient depth to ensure good coupling between the sensor and the surrounding soil (at least 1 ft. (0.3 m) deep with fully compacted soil on top). The wireless sensor unit with the three directional acquisition channels can record seismic energy in three Cartesian directions (vertical and two horizontal directions). The vibration signals obtained by the wireless accelerometer are acceleration time histories, which are processed in spectral domain using p-τ transformation, or slant-stack analysis [26].

Since passive sensing assumes the signals are random in nature and the analysis is done in the spectral domain, time sequence of the sampled data is not considered. Only the vertical direction has been used in the wave motion analysis for this study.

To monitor the responses of the reservoir throughout the CO_2 injection process, two linear test arrays were conducted at the Citronelle oil field. Each test array consists of 24 measurement points, which are all located near the oil wells. The site test layout is shown in **Figure 4**. The Line 1 is generally aligning with the north to south direction, whereas, Line 2 is in general in the northeast to southwest direction. Line 1 covered approximately a distance of 30,102 ft. (9175 m) in total with approximately 1309 ft. (399 m) for sensor spacing. Line 2 is 25,603 ft. (7804 m) in total span and has a sensor spacing of 1113 ft. (339 m) between pickup points. CO_2 is injected in well No. B-19-10 #2, which is located near the intersection of the two survey lines and is in the top north end of the Citronelle oil field. The sensors were buried at each measurement point, and the recording duration for each set was set at 39.06 s. The sampling frequency was set at 512 Hz.

Background measurement was deployed prior to the start of CO_2 injection in the field. It should be noted that in order to restore the pressure in the well to the level suitable for production, water injection at the well has been conducted since 2007. CO_2 injection in well No. B-19-10 #2 started in December 2009 and at the rate of 46.5 tons/day. The CO_2 injection was stopped from December 30, 2009 to January 26, 2010, due to the triplex pump not being able to maintain the injection pressure. After a thorough problem detection process, the pumping was resumed and, as a result, the average injection rate of CO_2 was stabilized at 31.5 tons/day. The CO_2 injection history in short tons until late September 2010 is presented in **Figure 5**. Final amount of CO_2 injected in the pilot well is about 8036 short tons. The record of well head pressure at Well

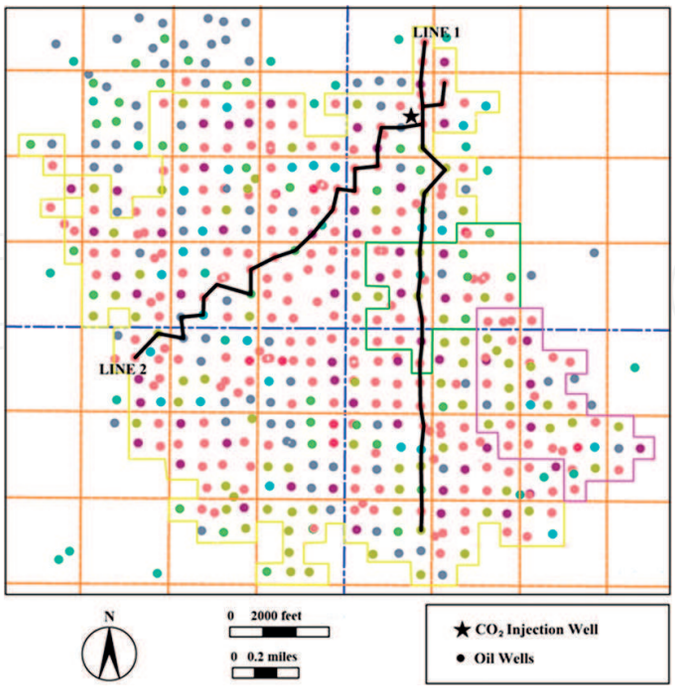

Figure 4. The testing lines at the Citronelle oil field.

http://dx.doi.org/10.5772/intechopen.78386

B-19-10 #2 from the beginning of CO_2 injection to the end of the injection is shown in **Figure 6**. The pressure has been normalized in order to compare it with the normalized stresses at the oil-bearing layer quantified based on the geophysical testing results to be presented later.

In the first month of CO_2 injection, the well head pressure changed from 2400 psig (16,547.4 kPA) to 3800 psig (26,200.1 kPA). After CO_2 injection was resumed on January 27, 2010, the range of well head is between 3800 psig (26,200.1 kPA) and 4200 psig (28,957.9 kPA). Passive tests were conducted at the Citronelle oil field in December 2009 when the start of significant CO_2 injection,

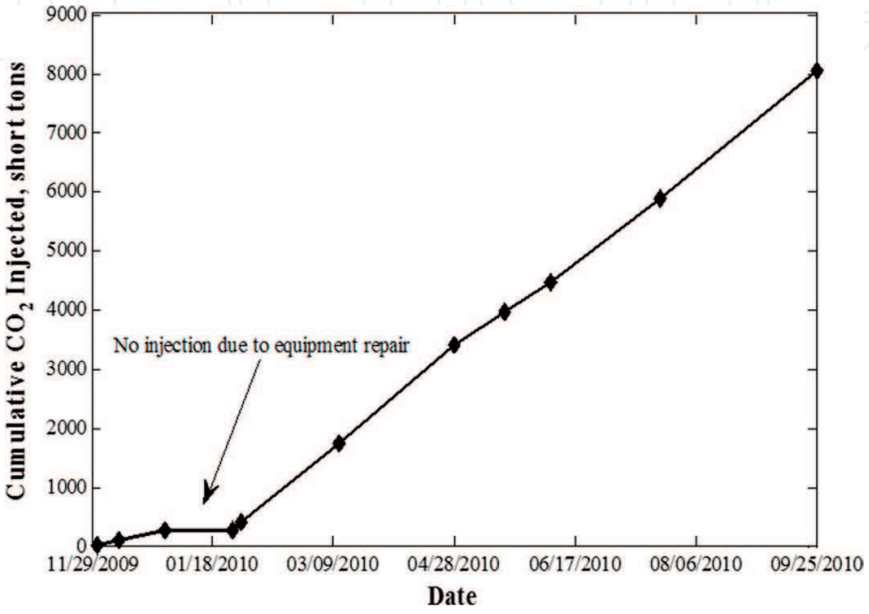

Figure 5. Record of CO_2 injection during Phase II at Well B-19-10#2.

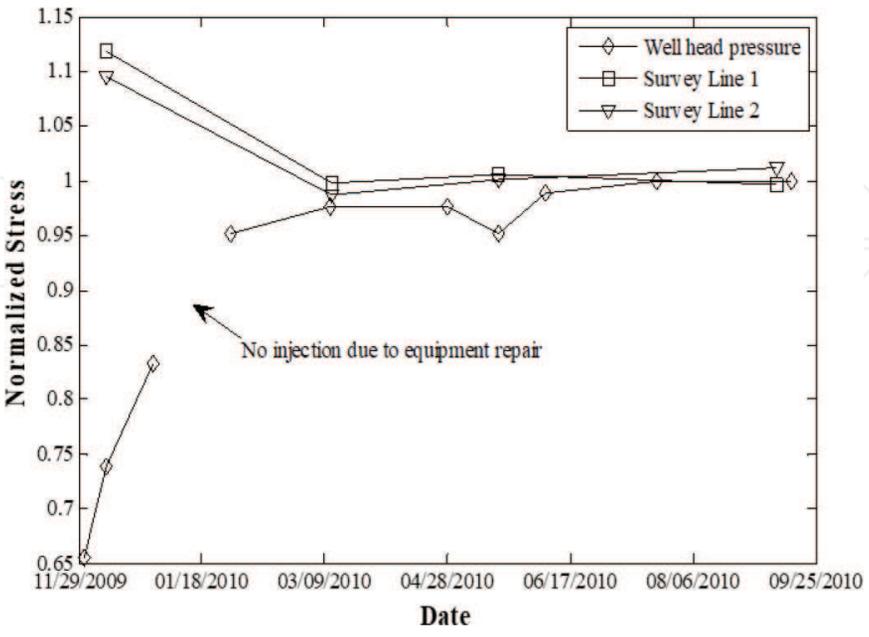

Figure 6. Normalized well head pressure at Well B-19-10#2 during CO_2 injection with geophysical test data.

and during steady CO_2 injection in March 2010, May 2010, and September 2010, respectively. Water injection was switched back immediately after CO_2 injection was completed. In addition, measurements were made after CO_2 injection in November 2010, March 2011, and May 2011, respectively. A summary of the monitoring history at the Citronelle oil field is shown in **Table 1**.

2.2. Injection history analysis

Since the monitoring process involved the three injection stages, namely, water injection (pressure building), CO_2 injection, and post-injection, it is of interest to interpret the results according to the stages. For each stage, at least three monitoring tests were performed. Hence, there are three test group data. To compare the field pressure responses at different injection stages, statistical parameters have been adopted including average shear-wave velocities and coefficient of variations.

Statistical analysis is performed first by determining the averaged shear-wave velocities at different strata for each test group along each of the test lines. The average wave velocities are defined as [27]:

$$\theta = \frac{1}{N}\sum_{i=1}^{N} x_i \tag{4}$$

where θ represents the average wave speed, x_i represents the wave speed data at the corresponding depth for each test group, and N represents the number of tests in each test group. After calculating the average shear-wave velocities, the standard deviations, α, of the corresponding data are determined as:

$$\alpha = \sqrt{\frac{1}{N}\sum_{i=1}^{N}(x_i - \theta)^2} \tag{5}$$

Test no.	Injection	Monitoring date
1	Water	8–10 October 2008
2	Water	21–22 January 2009
3	Water	15–16 June 2009
4	CO_2	9–10 December 2009
5	CO_2	11–12 March 2010
6	CO_2	18–19 May 2010
7	CO_2	8–9 September 2010
8	Water	17–18 November 2010
9	Water	16–17 March 2011
10	Water	17–18 May 2011

Table 1. Summary of monitoring history at the Citronelle oil field.

http://dx.doi.org/10.5772/intechopen.78386

The average and standard deviation values are then used to compute the coefficient of variation (COV), C_v:

$$c_v = \frac{\alpha}{\theta} \tag{6}$$

The coefficient of variation illustrates how far a set of numbers deviates from the average value—an indication of the consistency of the layer responses as well as the repeatability of the measurements. The CO_2 injection process instigated a continuous stress building within the oil-bearing layer at the Citronelle oil field. Due to the presence of the anhydrite layer, the CO_2 remains within the oil-bearing rock and will slowly flow into the oil-bearing rock resulting in the stress built-up dissipating throughout the oil-bearing layer. As long as the anhydrite retains its integrity and that there are no break-throughs within the rock medium, the pressure at the oil-bearing layer should be consistently higher than in the strata above. Thus, the stress wave velocity at the oil-bearing layer should be higher than in the strata above. The COV and average values of the wave speed profile will be used to determine the stress state in the strata system. **Table 2** lists the C_v values from both Line 1 and Line 2 tests. **Table 2** shows that the C_v values for each layer are reduced during the injection history, indicating a stressing of the strata.

The C_v values of the wave speed at the oil-bearing layer is an indication of the stabilization of the strata pressurization process: as the oil-bearing layer pressure is building up, a larger C_v value is expected, which dropped later indicating stable pressure in the oil-bearing rock.

Layer	Before CO_2 injection		During CO_2 injection		After CO_2 injection	
	Line 1	Line 2	Line 1	Line 2	Line 1	Line 2
1	0.05	0.06	0.03	0.07	0.02	0.05
2	0.06	0.06	0.09	0.11	0.01	0.07
3	0.08	0.07	0.06	0.18	0.02	0.03
4	0.16	0.08	0.05	0.20	0.01	0.05
5	0.15	0.08	0.10	0.17	0.03	0.04
6	0.13	0.05	0.14	0.15	0.03	0.04
7	0.16	0.07	0.14	0.14	0.01	0.03
8	0.14	0.03	0.15	0.14	0.02	0.01
9	0.13	0.05	0.11	0.11	0.01	0.03
10	0.17	0.05	0.04	0.09	0.01	0.03
11	0.16	0.06	0.05	0.06	0.01	0.04
12	0.08	0.05	0.07	0.06	0.002	0.02
13	0.04	0.06	0.05	0.03	0.004	0.003
14	0.07	0.03	0.06	0.05	0.01	0.001

Table 2. Summary of C_v values for results from both Line 1 and Line 2 tests.

Table 2 shows the C_v values for each layer and each survey line. The table shows that in all cases, C_v values are less than 0.2 indicating that the strata responses are slow, and consistent and that there are no drastic events occurring during the whole injection process. The C_v values also are consistently dropping during the three stages indicating that the pressurization is gradually stabilized during the process.

Careful evaluation of **Table 2** indicates that there is a difference between the results from both survey lines: for the after CO_2 injection stage, it is seen where the C_v value is shown to be 0.01 for Line 1 and the value is 0.001 for Line 2 (Layer 14). This is an order of magnitude different. For the before CO_2 injection (initial water pumping) stage, where the C_v value is 0.07 for Line 1 and is 0.03 for Line 2. This observation may be detrimental considering the experimental resolution of the geophysical testing method, which is discussed below.

3. Geophysical response analysis and interpretations

3.1. Shear-wave speed determination

As mentioned earlier, each test line has 24 measurements points representing a total of 24 channels in data processing. To process the shear-wave velocity data, SeisOpt ReMi software was used [26]. The procedure of stress wave signal processing involves first a wave field data transformation (ReMi Vspect module was used), which converts the time domain data acquired in the field to frequency domain. An interactive Rayleigh-wave dispersion modeling was then conducted with the outcomes is 1-D shear-wave velocity models. At the end, the dispersion curves were generated [28].

Figure 7 shows the typical averaged shear-wave velocity profiles as a function of depth (measured from Line 1 and Line 2). The shear-wave velocity curve was obtained based on the averaging of the test data sets during each test stage and is shown to have a total of 14 strata. The 14th strata correspond to the measurements of shear-wave velocity to depths at around 12,500 ft. (3810 m), which is about the oil-bearing Donovan sand. As described earlier, most of the injection pressures were retained within the oil layer at around 12,500 ft. (3810 m). Hence, the test results confirmed about the pressurization of the Donovan sand and that the anhydrite layer has maintained its leak prevention integrity.

In order to compare the changes of the shear-wave velocity obtained from the geophysical tests, the data were divided into three groups: before CO_2 injection, during CO_2 injection, and after CO_2 injection. **Figures 8–10** show the shear-wave velocity curves from both Line 1 and Line 2 tests for the three stages: **Figure 8** shows the results of average shear-wave velocity versus depth curve for test 1, test 2, and test 3 (before CO_2 injection) for Line 1 and Line 2, respectively. Error bars are used to indicate the deviation of shear-wave velocity in the measurements of each group.

Both Line 1 and Line 2 show that different strata experienced different stress histories: for Line 1, the top seven layers (approximately at 6000 ft. (1829 m) depth) are shown to experience

http://dx.doi.org/10.5772/intechopen.78386

initial increase in wave speed (during CO_2 injection) and then decreasing wave speed (after CO_2 injection); the trend reversed after 6000 ft. (1829 m) depth showing increasing wave speeds for both during and after CO_2 injections; and finally, the oil-bearing layer [around 12,000 ft. (3658 m) depth] showed slowly decreasing wave speeds. Line 2, on the other hand, showed an increase decrease trend up to 3000 ft. (914 m) depth; followed by an increasing pattern above the oil-bearing layer; and decreasing wave speeds at the oil-bearing layer. The explanation of the response history is that the oil-bearing layer experienced strata expansion due to the injection pressure and the inability of oil to escape quick enough from the oil sand; hence, the pressure is transferred to the strata above the oil-bearing layer (mostly salient saturated material), which experienced stressing (increasing wave speed). This trend reversed for the upper layer above the salient layers, which is dependent upon the balancing act of the weight of the overburden and the upward lifting of the injection pressure.

Figure 9 shows the results of average shear-wave velocity versus depth curve for test 4, test 5, test 6, and test 7 (during CO_2 injection) for Line 1 and Line 2, respectively. Wave speeds results of the last four layers shown in **Figure 9** are higher than the corresponding results shown in **Figure 8**. The increase in shear-wave velocity is associated with CO_2 injection, which caused an increase in the effective stresses in layers above the injection zone (pressurization). **Figure 10** shows the results of average shear-wave velocity versus depth curve for test 8, test 9, and test 10 (after CO_2 injection) for Line 1 and Line 2, respectively. The deviations on the graphs shown in **Figure 10** are significantly smaller when compared to **Figures 8** and **9** indicating that the strata pressurization has stabilized.

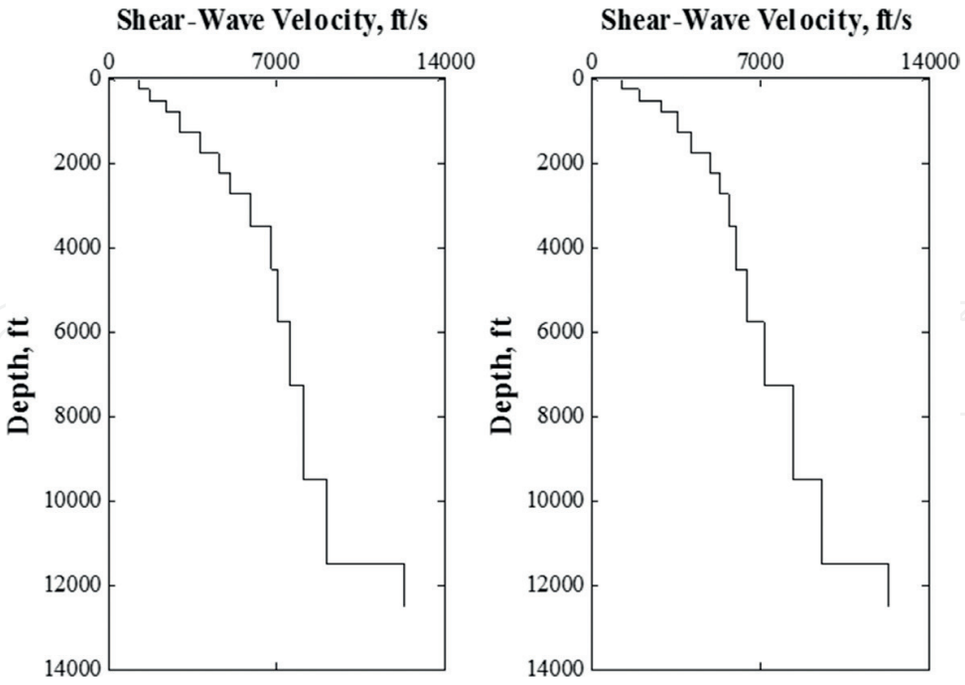

Figure 7. Average shear-wave velocity profiles versus depth from sensor survey Line 1 (left) and Line 2 (right), September 8–9, 2010.

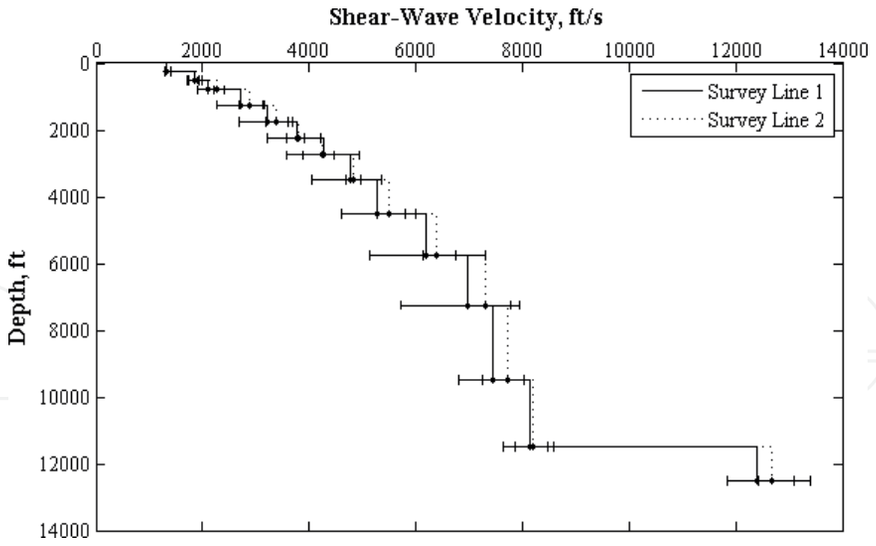

Figure 8. Average shear-wave velocity profile versus depth before CO_2 injection, average of test 1, test 2, and test 3 (Line 1 and Line 2).

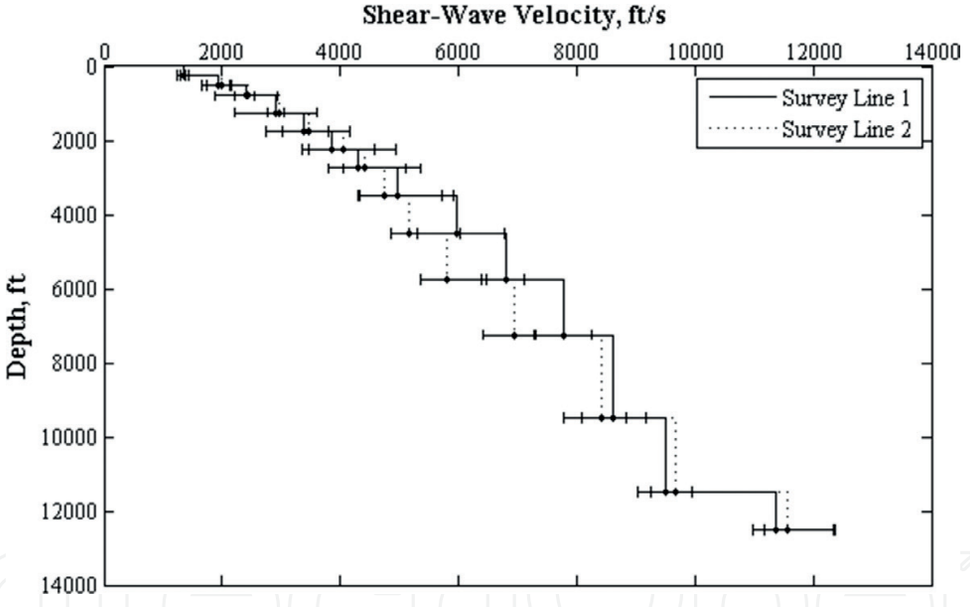

Figure 9. Average shear-wave velocity profile versus depth before CO_2 injection, average of test 4, 5, 6, and 7 (Line 1 and Line 2).

It is important to point out that the test line selection is constrained by available monitoring sites and is selected in order to help determine possible directional effects of the CO_2 migration at the oil field. Hence, the first test line would determine the likely CO_2 migration in the north-east direction, and the second test line would determine the flow in the northeast and southwest directions. When comparing the average velocity at the oil-bearing layer, the results from Line 1 indicates that the wave speed has reached 12,392 ft./s (3,777 m/s) during water injection, 11,365 ft./s (3,464 m/s) during CO_2 injection, and has dropped slightly to 11,109 ft./s (3,386 m/s) after the CO_2 injection. This indicates that there is a possibility that the supercritical CO_2 may be migrating slowly in the north-east direction.

http://dx.doi.org/10.5772/intechopen.78386

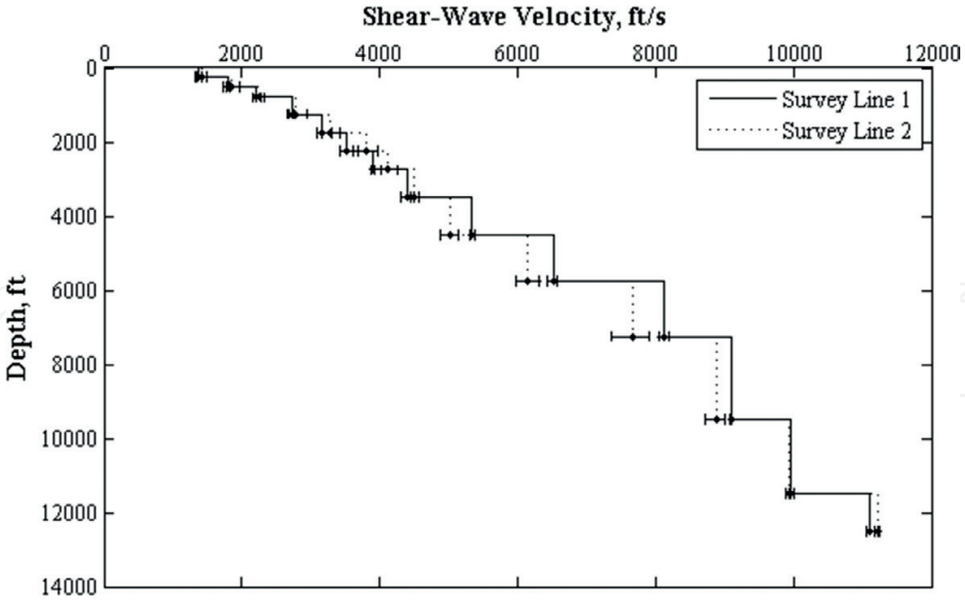

Figure 10. Average shear-wave velocity profile versus depth during CO_2 injection, average of test 8, test 9, and test 10 (Line 1 and Line 2).

On the other hand, Line 2 has wave velocity reaching 12,667 ft./s (3,861 m/s) during water injection, 11,570 ft./s (3,527 m/s) during CO_2 injection, which has dropped to 11,236 ft./s (3,425 m/s) post CO_2 injection. Again, there is a possibility of mobilization of oil/CO_2 flow—a likelihood of enhanced oil production in the months to come.

It is noticed that the strata pressure above the oil-bearing layer is slow in building up as it takes time for the pressure to dissipate into the upper strata. To study this effect, the wave speed responses above the oil-bearing layers are studied: it is shown for Line 1, the wave speed above the oil-bearing layer has increased from 8144.6 ft./s (2,482.5 m/s) initially, to 9512.9 ft./s (2,899.5 m/s) during CO_2 injection, and finally, increased to 9963.7 ft./s (3,036.9 m/s) post-injection. This indicates a slow building up of pressure. For Line 2, the wave speed immediately above the oil-bearing layer has increased from 8207.6 ft./s (2,501.7 m/s) before injection to 9664.0 ft./s (2,945.6 m/s) during CO_2 injection, and finally, to 9935.8 ft./s (3,028.4 m/s) post-injection. The interpretation of this observation is that the oil pressure is pushing against the strata above the Donovan sand and has resulted in the strata pressurization. It is concluded that the pressure build-ups are almost identical in both directions indicating uniform build-up of pressures at all directions at the Citronelle oil field.

3.2. Discussion on geophysical sensing for CO_2 injection studies

Geophysical testing has been applied to projects similar to the Citronelle field study for the purposes of determining production induced stress changes in the oil-bearing strata and site anisotropy changes. In most high-resolution seismic detections, the tests are performed with controlled excitations such as the use of explosions, seismobile vibrations, or gun shots. The results have sensitivities that can indicate possible migration of injected fluids. However, the interpretation of strata stress changes based on wave speed changes is inherently challenging, as a result of the constrained temporal and spatial resolutions. As a result, the

velocity change ratio function $(\Delta v/v)$ has been suggested as a means to establish the detection of geomechanical condition changes due to oil production or fluid injection [29] and has been successfully implemented in a study to synchronized field measurements to localized microtremors [30].

To determine the stress wave speed changes, the velocity change functions are computed for before, during and after CO_2 injection:

$$\left(\frac{\Delta v}{v}\right)_i = \frac{(v_{During})_i - (v_{Before})_i}{(v_{Before})_i} \tag{7}$$

$$\left(\frac{\Delta v}{v}\right)_i = \frac{(v_{After})_i - (v_{Before})_i}{(v_{Before})_i} \tag{8}$$

$$\left(\frac{\Delta v}{v}\right)_i = \frac{(v_{after})_i - (v_{during})_i}{(v_{during})_i} \tag{9}$$

Figure 11 shows $(\Delta v/v)$ for different stages of the injection process at Citronelle field indicating different strata stress plays: for both Line 1 and Line 2, it is shown that the stress waves have reduced in the injection layer (Layer 14) after CO_2 injection indicating that the CO_2 gas may have migrated at this stage. The velocity change functions for Layers 8–10 (corresponding to

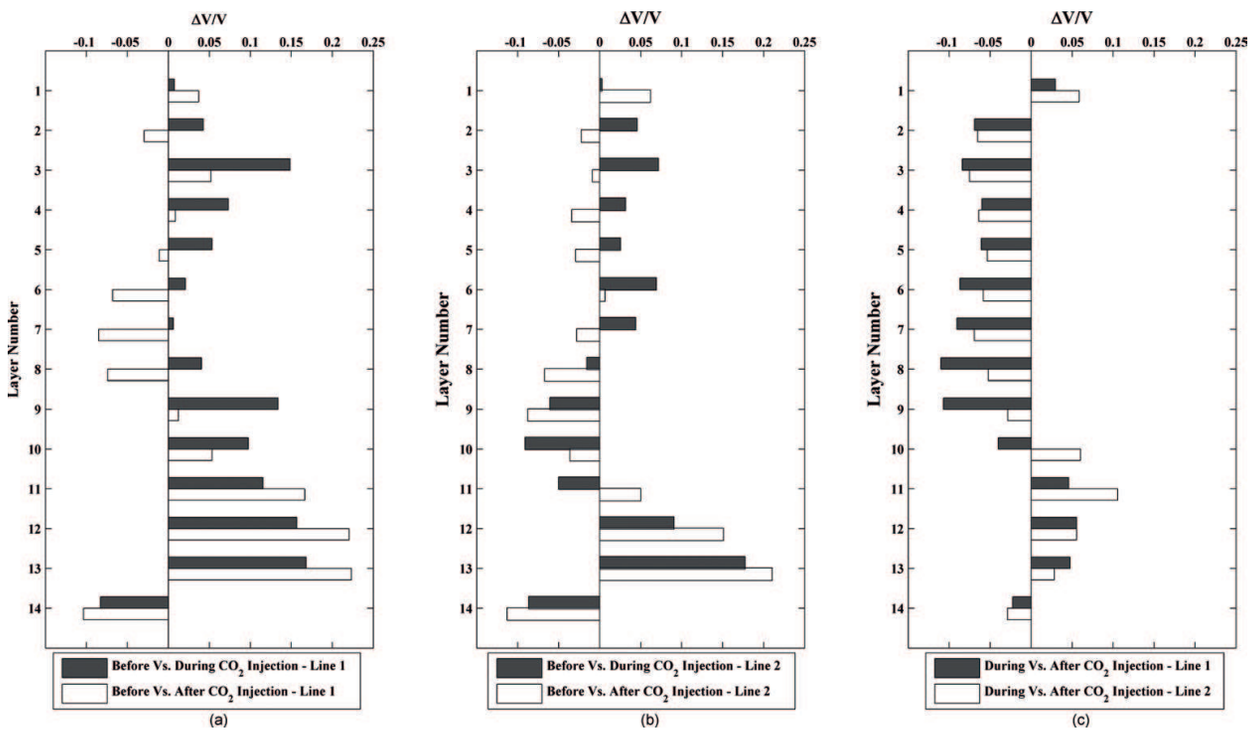

Figure 11. Velocity change functions vs. strata layers for (a) injection histories for Line 1; (b) injection histories for Line 2 and (c) injection histories for Line 1 and Line 2.

http://dx.doi.org/10.5772/intechopen.78386

salient layer) are negative, most likely indicating a reduction in effective stress. Following Eq. (1), this may be interpreted as an increase in pore water pressure in the salient formation.

The last figure in **Figure 11** shows a comparison between Line 1 and Line 2 using Eq. (9). This figure shows that the two trends are in consistent in general and that both show the same trend of velocity increase right above the oil production strata (which shows negative velocity change functions). This further enhances the interpretation that the stress within the injection may be reduced due to migration of CO_2 plum.

A reduction of the strata pressure (shear-wave velocity) could mean a likely leak occurs within the system, which has not been identified at the Citronelle field. The shear-wave velocities at the Donovan oil-bearing layer are normalized by their average value and are plotted against the normalized well head pressure in **Figure 6**. Assuming the shear-wave velocity is a good representation of the stress level within the oil-bearing stratum, the well-fitting of the two sets of data represents that the geophysical testing method has accurately quantified the stresses within the reservoir.

4. Conclusions

Carbon sequestration through injection into a depleted oil field is an effective method to reduce atmospheric CO_2. However, proper monitoring of the CO_2 injection process is essential in order to ensure the geomechanical stability of the storage reservoir and to minimize risks of potential geohazard to the terrestrial and sub-terrestrial environments. This chapter reports the use of a passive microseismic sensing technique to monitor the CO_2 injection process at the Citronelle oil field, Alabama. The ability of the passive DoReMi technique to monitor the CO_2 sequestration process in the heterogeneous oil reservoir is demonstrated through analysis of the wave speed profiles indicating that there are strata stress build-ups during and after the injection of CO_2, which resulted in the pressurization of the Rodessa oil-bearing layers. Clear demarcation of the shear-wave velocity profile is shown for before, during, and after the CO_2 injection in the field. The detection of geomechanical deformation within the overburden of the reservoir is important for monitoring the long-term CO_2 storage—continued monitoring may provide information on possible reservoir breakthroughs and possible pathways for CO_2 leakage.

The COV value associated with the shear-wave velocity changes is suggested as a measure of the conditions at the oil field and is observed to drop in value during the CO_2 injection process, indicating that the stress state in the oil-bearing layer has reached a stable state. Thus, the COV values can be used as an indication of oil field stability during the CO_2 injection operation and have the potential for long-term monitoring of the strata stress change throughout the field operations. Further studies are needed to develop the COV value into risk index that can be used to indicate geohazard. The strata stressing is especially important to the City of Citronelle, where the oil wells (potential CO_2 leak sites) are in close vicinity to humans and livestock. Continued geophysical monitoring of the strata stress changes can help mitigate potential geohazards due to the CO_2 injection operation.

Acknowledgements

This work is supported by the US Department of Energy (USDOE), National Energy Technology Laboratory (NETL) under Cooperative Agreement No. DE-FC26-06NT43029 with the University of Alabama at Birmingham. The work is also supported by Denbury Resources, Southern Company, the Geological Survey of Alabama, the University of Alabama, the Alabama A and M University, and the University of North Carolina at Charlotte. The first author is also supported by the Doctoral Foundation of Henan Polytechnic University (B2015–78).

The authors would also like to acknowledge the technical supports and advices from Dr. Peter M. Walsh from the University of Alabama at Birmingham, Dr. Richard A. Esposito of Southern Company, Dr. Jack C. Pashin of the Geological Survey of Alabama and Mr. Gary N. Dittmar of Denbury Resources. The Technical assistance from Dr. Satish Pullammanappallil from Optim, Inc. is also greatly appreciated.

The views, opinions, findings, and conclusions reflected in this publication are the responsibility of the authors only and do not represent the official policy or position of the USDOE, NETL, or any State or other entity.

Author details

Shen-En Chen[1]* and Yangguang Liu[2]

*Address all correspondence to: schen12@uncc.edu

1 University of North Carolina at Charlotte, Charlotte, NC, USA

2 School of Resources and Environment, Collaborative Innovation Center of Coalbed Methane and Shale Gas for Central Plains Economic Region, Henan Polytechnic University, Jiaozuo, Henan Province, China

References

[1] Halmann MM, Steinberg M. Greenhouse Gas Carbon Dioxide Mitigation: Science and Technology. Boca Raton, FL: Lewis Publishers; 1999

[2] Balat M, Balat H, Acici N. Environmental issues relating to greenhouse carbon dioxide emissions in the world. Energy Exploration & Exploitation. 2003;**21**(5-6):457-473

[3] Zhong WY, Haigh JD. The greenhouse effect and carbon dioxide. Weather. 2013;**68**(4): 100-105

[4] White CM, Strazisar BR, Granite EJ, Hoffman JS, Pennline HW. Separation and capture of CO_2 from large stationary sources and sequestration in geological formations—Coalbeds

and deep saline aquifers. Journal of the Air & Waste Management Association. 2003;**53**(6):645-715

[5] Bachu S. CO_2 storage in geological media: Role, means, status and barriers to deployment. Progress in Energy and Combustion Science. 2008;**34**(2):254-273

[6] Holloway S. Underground sequestration of carbon dioxide—A viable greenhouse gas mitigation option. Energy. 2005;**30**(11-12):2318-2333

[7] Plasynski SI, Litynski JT, McIlvried HG, Srivastava RD. Progress and new developments in carbon capture and storage. Critical Reviews in Plant Sciences. 2009;**28**(3):123-138

[8] Lake LW. Enhanced Oil Recovery. Englewood Cliffs, NJ: Prentice Hall; 1989

[9] Blunt M, Fayers FJ, Orr FM. Carbon dioxide in enhanced oil recovery. Energy Conversion and Management. 1993;**34**(9-11):1197-1204

[10] Gaspar Ravagnani ATFS, Ligero EL, Suslick SB. CO_2 sequestration through enhanced oil recovery in a mature oil field. Journal of Petroleum Science and Engineering. 2009;**65**(3-4):129-138

[11] Koottungal L. Special report: 2010 worldwide EOR survey. Oil and Gas Journal. 2010;**108**(14):41-53

[12] Hosa A, Esentia M, Stewart J, Haszeldine S. Injection of CO_2 into saline formations: Benchmarking worldwide projects. Chemical Engineering Research and Design. 2011;**89**(9):1855-1864

[13] Rutqvist J, Vasco DW, Myer L. Coupled reservoir-geomechanical analysis of CO_2 injection and ground deformations at in Salah, Algeria. International Journal of Greenhouse Gas Control. 2010;**4**(2):225-230

[14] Morris JP, Hao Y, Foxall W, McNab W. In Salah CO_2 storage JIP: Hydromechanical simulations of surface uplift due to CO_2 injection at in salah. Energy Procedia. 2011;**4**:3269-3275

[15] Onuma T, Okada K, Otsubo A. Time series analysis of surface deformation related with CO_2 injection by satellite-borne SAR interferometry at in Salah, Algeria. Energy Procedia. 2011;**4**:3428-3434

[16] Chadwick RA, Arts R, Bentham M, Eiken O, Holloway S, Kirby GA, Pearce JM, Williamson JP, Zweigel P. Review of monitoring issues and technologies associated with the long-term underground storage of carbon dioxide. Geological Society, London, Special Publications. 2009;**313**(1):257-275

[17] White D. Monitoring CO_2 storage during EOR at the Weyburn-Midale Field. The Leading Edge. 2009;**28**(7):838-842

[18] Arts R, Eiken O, Chadwick A, Zweigel P, Van Der Meer L, Zinszner B. Monitoring of CO_2 injected at Sleipner using time lapse seismic data. Energy. 2004;**29**(9-10):1383-1392

[19] Giese R, Henninges J, Lüth S, Morozova D, Schmidt-Hattenberger C, Würdemann H, Zimmer M, Cosma C, Juhlin C. Monitoring at the CO_2 SINK site: A concept integrating geophysics, geochemistry and microbiology. Energy Procedia. 2009;**1**(1):2251-2259

[20] Esposito RA, Pashin JC, Walsh PM. Citronelle dome: A giant opportunity for multi-zone carbon storage and enhanced oil recovery in the Mississippi interior Salt Basin of Alabama. Environmental Geosciences. 2008;**15**(2):53-62

[21] Esposito R, Pashin J, Hills D, Walsh P. Geologic assessment and injection design for a pilot CO_2-enhanced oil recovery and sequestration demonstration in a heterogeneous oil reservoir: Citronelle field, Alabama, USA. Environmental Earth Sciences. 2010;**60** (2):431-444

[22] Hawkins K, Howe S, Hollingworth S, Conroy G, Ben-Brahim L, Tindle C, Taylor N, Joffroy G, Onaisi A. Production-induced stresses from time-lapse time shifts: A geomechanics case study from Franklin and Elgin fields. The Leading Edge. 2007:655-662

[23] Maxwell SC, Urbancic TI. The role of passive microseismic monitoring in the instrumented oil field. The Leading Edge. 2001;**20**(6):636-639

[24] Verdon JP, Kendall J-M, White DJ, Angus DA, Fisher QJ, Urbancic T. Passive seismic monitoring of carbon dioxide storage at Weyburn. The Leading Edge. 2010;**29**(2):200-206

[25] Chen S-E, Liu Y, Wang P. DoReMi—A passive geophysical monitoring technique for CO_2 injection. In: Proceedings of the SPE Eastern Regional Meeting 2011, August 17-19, 2011. Columbus, OH, USA: Society of Petroleum Engineers (SPE); 2011. pp. 254-266

[26] Optim. User's Manual: SeisOpt ReMi Version 4.0. Reno, NV: Optim, Inc; 2006

[27] Rétháti L. Probabilistic Solutions in Geotechnics. Elsevier Science; 1988

[28] Louie JN. Faster, better: Shear-wave velocity to 100 meters depth from refraction microtremor arrays. Bulletin of the Seismological Society of America. 2001;**91**(2):347-364

[29] Hatchell P, Sayers C, van den Beukel A, Molenaar M, Maron K, Kenter C, Stammeijer J, van der Valde J. Whole Earth 4D: Monitoring geomechanics, Extended Abstract. In: 73rd SEG Meeting; Dallas, USA; 2003. pp. 1330-1333

[30] Steiner B, Saenger EH, Schmalholz SM. Time reverse modeling of low-frequency microtremors: Application to hydrocarbon reservoir localization. Geophysical Research Letters. 2008;**35**(3):L03307